J Therm Anal Calorim (2011) 105:145–150
DOI 10.1007/s10973-010-1267-x

# Thermogravimetric analysis of walnut shell as pyrolysis feedstock

**Korkut Açıkalın**

Received: 26 October 2010 / Accepted: 14 December 2010 / Published online: 5 January 2011


**Abstract** Thermal degradation behavior and kinetics of a biomass waste material, namely walnut shell, were investigated by using a thermogravimetric analyzer. The desired final temperature of 800 °C was achieved at three different heating rates (2, 10, and 15 °C $min^{-1}$) under nitrogen flow (50 mL $min^{-1}$). The TG and DTG curves exhibited three distinct zones that can mainly be attributed to removal of water, decomposition of hemicellulose + cellulose, and decomposition of lignin, respectively. The kinetic parameters (activation energy, pre-exponential factor, and reaction order) of active pyrolysis zone were determined by applying Arrhenius, Coats–Redfern, and Horowitz–Metzger methods to TG results. The values of activation energies were found to be between 45.6 and 78.4 kJ $mol^{-1}$. There was a great agreement between the results of Arrhenius and Coats–Redfern methods while Horowitz–Metzger method yielded relatively higher results. The existence of kinetic compensation effect was evident.

**Keywords** TG · Walnut shell · Pyrolysis kinetics · Coats–Redfern · Horowitz–Metzger

## Introduction

Depletion of fossil fuels and environmental problems due to their usage caused an increasing worldwide interest on search for alternative and renewable energy sources. Among the potential renewable energy sources, biomass is recognized as the most promising one owing to its unique properties such as availability, easy processability, and being environmentally friendly. At present, biomass is the fourth largest energy source in the world after coal, oil, and natural gas, and provides 10.1% of primary energy consumption [1]. The worldwide availability of biomass is predicted as 220 billion ton per year corresponding to 4500 EJ ($10^{18}$ J) [2]. Biomass sources, unlike fossil fuel sources, are evenly distributed over earth's surface. Thus, their usage contributes to energy source decentralization, and strongly encourages the nations to be energy self-sufficient. The processability of biomass to obtain fuels and chemicals is easier compared to coal due to its higher reactivity and volatility [3, 4]. Another uniqueness of biomass lies on being the one and only renewable energy source that can be converted to liquid, solid, and gaseous fuels [5]. Finally, biomass is an ecofriendly energy source. It does not contribute to $CO_2$ build up and related problems [6] since it fixes the $CO_2$ amount by photosynthesis.

Biomass materials can be converted to chemicals and/or fuels by using thermochemical conversion processes. Pyrolysis is one of these processes, and appears to be the most promising conversion route. In pyrolysis, biomass is heated to moderate temperatures (400–600 °C) in the absence of oxygen to produce liquid, solid, and gaseous products. In literature, it is reported that the liquid product of pyrolysis process can be used as a feedstock in existing petroleum refineries [7]. However, the development of technically and economically feasible systems for conversion processes requires a fundamental understanding of thermal properties and reaction kinetics related to feedstock.

Thermoanalytical techniques are the most common tools for studying the thermal characteristics and kinetics of biomass pyrolysis. Thermogravimetric (TG) analysis is one of these techniques in which the mass loss of a sample is

K. Açıkalın (✉)
Chemical Engineering Department, Yıldız Technical University, Davutpaşa Cad. No:127, Esenler, 34210 Istanbul, Turkey
e-mail: korkut.acikalin@gmail.com

measured against temperature under controlled heating rate and gas atmosphere, and then recorded in the form of TG curves [8]. TG can be run in either isothermal or non-isothermal (dynamic) mode. Non-isothermal TG is widely preferred since it requires fewer data than isothermal TG [9]. Differential thermogravimetric (DTG) analysis curves are also valuable tools for kinetic calculations, and are derived from TG curves.

This study aims to provide a clear understanding of thermal degradation characteristics and kinetics of a biomass waste material, namely walnut shell. For this purpose, TG was performed at different heating rates, and the kinetic parameters (activation energy, pre-exponential factor, and reaction order) were calculated by various methods such as Arrhenius, Coats–Redfern, and Horowitz–Metzger.

## Materials and methods

### Materials

In this work, walnut shell was subjected to TG. Walnuts were obtained from a local market (Edirne, Turkey) and their shells were gently separated from the fruit. Shell samples were ground to particle size <0.1 mm by using Ika A11 model analytic mill. The samples were dried under vacuum at 105 °C, and kept in glass containers. The proximate and ultimate analysis data for walnut shell are given in Table 1.

### TG analysis

The Perkin Elmer Diamond TG/DTA system was used to measure and record the mass change with temperature of the sample over the course of the pyrolysis reaction. The runs were carried out non-isothermally at three different heating rates (2, 10, and 15 °C $min^{-1}$). Nitrogen was used as the carrier gas, at a flowrate of 50 mL $min^{-1}$. A sample mass of 5 ± 0.4 mg was used in each experiment. Open platinum sample pans were used as sample holders. The tests were conducted in a wide temperature range from 50 to 800 °C.

**Table 1** Proximate and ultimate analysis of walnut shell

| Proximate analysis/% | | | | | Ultimate analysis/% | | | | |
|---|---|---|---|---|---|---|---|---|---|
| M | VM | FC | Ash | HHV | C | H | O | N | S |
| 2.57 | 78.04 | 18.75 | 0.64 | 4265 | 48.34 | 6.16 | 44.78 | 0.69 | 0.03 |

*M* Moisture, *HHV* higher heating value/kcal $kg^{-1}$, *VM* volatile matter, *FC* fixed carbon; *VM*, *FC* ash values are in dry basis; Oxygen amount is calculated by difference

### Kinetic modeling

Pyrolysis of biomass is a solid phase degradation reaction and can be represented by the reaction scheme in which biomass degrades thermally, and forms solid residue (char) and volatiles [10]. The rate equation of pyrolysis can be described as follows:

$$\frac{d\alpha}{dt} = kf(\alpha), \tag{1}$$

where $k$ is the rate constant, $f(\alpha)$ is the reaction model, and $\alpha$ is the conversion (or degradation) rate. Equation 1 expresses the rate of pyrolysis, $d\alpha/dt$, at a constant temperature as a function of the reactant conversion and rate constant. Conversion is described as follows:

$$\alpha = \frac{(W_0 - W_t)}{(W_0 - W_f)}, \tag{2}$$

where $W_0$, $W_f$, and $W_t$ are initial, final, and time $t$ masses of the sample, respectively. By replacing the rate constant with Arrhenius equation, and choosing $n$th order reaction model Eq. 1 becomes

$$\frac{d\alpha}{dt} = Ae^{\left(-\frac{E}{RT}\right)}(1-\alpha)^n, \tag{3}$$

where $A$ is the pre-exponential (or frequency) factor, $E$ is the activation energy and $R$ is the universal gas constant. Since the studies were done non-isothermally, introducing the heating rate ($\beta = dT/dt$) to Eq. 3, and rearranging leads to the final form of rate equation

$$\frac{d\alpha}{(1-\alpha)^n} = \left(\frac{A}{\beta}\right)e^{\left(\frac{-E}{RT}\right)}dT. \tag{4}$$

Equation 4 is the fundamental expression of analytical methods to calculate kinetic parameters for $n$th order reactions on the basis of TG data as mentioned in other studies [11, 12].

## Results and discussion

### TG/DTG curves

Figure 1 shows the TG and the DTG curves of walnut shell at different heating rates as function of temperature. Based on the TG curves, the mass loss range can be divided into three zones since every single slope change on a TG curve indicates the beginning of a new zone. The first zone starts at 50 °C and finishes at the 175–205 °C interval with respect to the applied heating rate. This zone represents a slight mass loss (3.3–4.4%) which is due to the removal of water present in material and external water bounded by surface tension. The corresponding area on the DTG curve

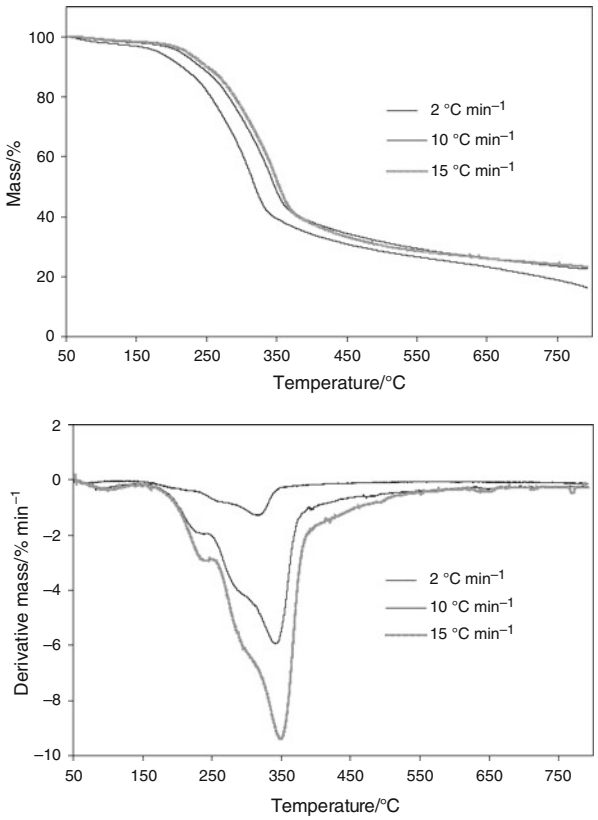


**Fig. 1** TG (*upper*) and DTG curves of walnut shells at different heating rates

is the small peak on the most left hand side. Following the TG curve, a "\"-shaped second zone is clearly seen in which a huge mass loss takes place. This zone represents the main devolatilization step of biomass pyrolysis, and is referred as active pyrolysis zone since mass loss rate is high. It starts at around 190 °C and ends at around 380 °C with an average mass loss of 56%. The corresponding area on the DTG curve is represented by an overlapping peak. The small shoulder at around 235 °C shows the presence of a minor reaction, and is followed by a major reaction which occurs as an intensive peak at around 335 °C. These thermal behaviors can be explained by the components of walnut shell. Walnut shell is mainly composed of hemicellulose, cellulose, and lignin like all other lignocellulosic materials. The thermogravimetric behavior of individual components have been well studied, and it is known that hemicellulose, cellulose, and lignin complete their decomposition at temperature intervals of 210–325, 310–400, and 160–900 °C, respectively [13–17]. Based on these information, the minor and major reactions observed in active pyrolysis zone can mainly be attributed to hemicellulose and cellulose decomposition, respectively. The third zone starts at around 380 °C and continues to 800 °C, and it is seen as a tailing in both TG and DTG curves. This zone is referred as passive pyrolysis zone since mass loss is smaller, and the mass loss rate is much lower compared to that in the second zone. Average mass loss was determined as 19%. This zone can be identified as that of lignin decomposition since the decomposition of lignin is known to occur slowly in a broad temperature range [18]. The average residual mass was determined as 21% at the end of the overall thermal degradation process. By considering the pieces of information given above, and with the knowledge of lignin yields its ~40% as a residue at the end of the pyrolysis process; the lignin and holocellulose (hemicellulose + cellulose) ratios of walnut shell can be estimated as 31% and 64%, respectively. The remaining part (5%) can be attributed to extractives and moisture.

The characteristic values related to active pyrolysis zone such as starting temperature ($T_i$), ending temperature ($T_f$), mass loss, maximum mass loss rate ($W_{max}$), and the temperature where this rate occured ($T_{max}$) was exactly determined for all studied heating rates since this zone was subjected to kinetic calculations. The values are given in Table 2. It can be clearly said that all characteristic temperatures increased with increasing heating rate. This situation can be assigned to combined effects of heat transfer at different heating rates and decomposition kinetics resulting in delayed decomposition [19]. Maximum mass loss rates were also shifted to higher temperatures with increasing heating rate as a consequence of the increasing effect of the inertia of devolatilization process as the characteristic time of the process is decreased [20].

## Calculation of kinetic parameters

Modeling of a reaction for biomass pyrolysis process is complicated because several parallel and serial reactions occur simultaneously. However, with the assumption that biomass undergoes a thermal degradation in any particular but clearly defined temperature zone as a single step irreversible reaction of *n*th order, Eq. 4 can be used to express the reaction rate. The present work aims to study the kinetics of active pyrolysis zone which is explained thoroughly in the previous section. The kinetics of active

**Table 2** Properties of active pyrolysis zone at different heating rates

| Property | Heating rate/°C min$^{-1}$ | | |
|---|---|---|---|
| | 2 | 10 | 15 |
| $T_i$/°C | 175 | 200 | 205 |
| $T_f$/°C | 346 | 377 | 389 |
| $T_{max}$/°C | 318 | 345 | 351 |
| $W_{max}$/% min$^{-1}$ | 1.27 | 5.89 | 9.36 |
| Mass loss/% | 55.49 | 55.46 | 57.50 |

pyrolysis zone was studied at 0.1–0.9 conversion interval in which the minor reaction was excluded so that the above assumption was provided. Mathematical calculations were performed by differential method of Arrhenius and integral methods of Coats–Redfern and Horowitz–Metzger.

In Arrhenius method, the final rate equation given below is obtained by linearization of Eq. 4 and making some rearrangements

$$\ln\left(\frac{\mathrm{d}\alpha}{\mathrm{d}T}\right) - n\ln(1-\alpha) = \ln\left(\frac{A}{\beta}\right) - \frac{E}{RT}. \quad (5)$$

The plot of $\ln(\mathrm{d}\alpha/\mathrm{d}T) - n\ln(1-\alpha)$ versus $(1/T)$ should give a straight line for the correct value of reaction order $n$. Hence, several values of $n$ were considered, the plots were drawn, and the related correlation coefficients ($R^2$) were calculated to generate $R^2$–$n$ curves (Fig. 2). Most appropriate $n$ ($n$ ensuring the highest $R^2$) values were determined from these curves for all studied heating rates. Using these values of $n$, final plots were generated (Fig. 3). The activation energy and pre-exponential factors were calculated from slope ($-E/R$) and interception ($\ln(A/\beta)$), respectively. The results are given in Table 3. Note that kinetic parameters could not be calculated for 2 °C min$^{-1}$ heating rate since the plot consisted of too many points, and formed a thick line which resulted in a $R^2$–$n$ line instead of a $R^2$–$n$ curve. In other words, $R^2$ showed a continuous increase with increasing $n$ values, and a proper reaction order could not be determined.

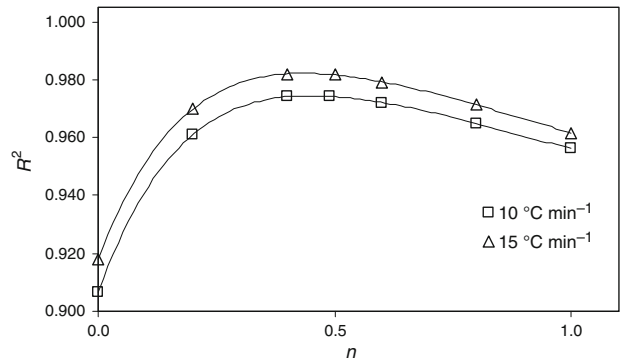


**Fig. 2** $R^2$–$n$ curves obtained by Arrhenius method

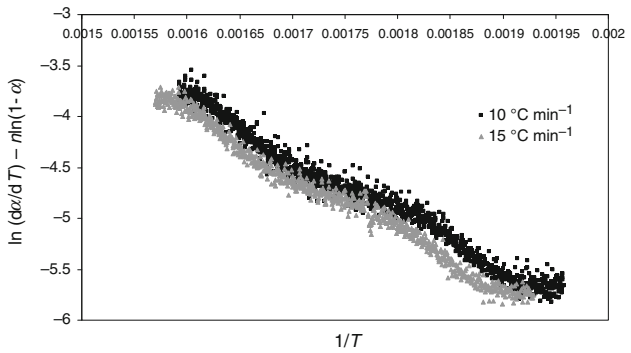


**Fig. 3** $\ln(\mathrm{d}\alpha/\mathrm{d}T) - n\ln(1-\alpha)$ versus $(1/T)$ plot for Arrhenius method

In Coats–Redfern method, Eq. 4 is integrated and the resulting exponential integral is approximated by the use of asymptotic series expansion [21]. The linearized final form is given as [22]:

$$\ln g(\alpha) = -\frac{E}{RT} + \ln\left(\frac{AR}{\beta E}\right) \quad (6)$$

where $g(\alpha) = -(\ln(1-\alpha))/T^2$ if $n = 1$; $g(\alpha) = (1-(1-\alpha)^{(1-n)})/((1-n)T^2)$ if $n \neq 1$. In this method, the correct reaction order is presumed to give the best linear plot of $\ln g(\alpha)$ versus $(1/T)$. So, the appropriate $n$ values were determined from $R^2$–$n$ curves (Fig. 4). Using these $n$ values final plots were generated (Fig. 5). The activation energy and pre-exponential factor values were determined from slope ($-E/R$) and interception ($\ln((AR)/(\beta E))$), respectively. The results are given in Table 4.

In Horowitz–Metzger method, the linearized form of final equation is given as [12]:

$$\ln g(\alpha) = \left(\frac{E\Phi}{RT_{\max}^2}\right) + \ln\left(\frac{ART_{\max}^2}{\beta E}\right) - \frac{E}{RT_{\max}} \quad (7)$$

where $\Phi = T - T_{\max}$, and $T_{\max}$ is the temperature in which maximum mass loss rate occurs. Here, $g(\alpha) = -\ln(1-\alpha)$ if $n = 1$; $g(\alpha) = (1-(1-\alpha)^{(1-n)})/(1-n)$ if $n \neq 1$. In this method, $\ln g(\alpha)$ versus $\Phi$ plot should be a straight line if $n$ is properly selected. The proper $n$ values were determined from $R^2$–$n$ curves (Fig. 6). Using these $n$ values final plots were drawn (Fig. 7). The activation energy and pre-exponential factors were determined from slope ($E/(RT_{\max}^2)$) and intercept ($\ln((ART_{\max}^2)/(\beta E)) - E/(RT_{\max})$), respectively. The results are shown in Table 5.

**Table 3** Kinetic parameters calculated from Arrhenius method

| $B$/°C min$^{-1}$ | $E$/kJ mol$^{-1}$ | Log $A$/min$^{-1}$ | Plot equation | $R^2$ | $n$ |
|---|---|---|---|---|---|
| 10 | 45.7 | 3.15 | $y = -5497.3x + 4.948$ | 0.9745 | 0.45 |
| 15 | 47.7 | 3.43 | $y = -5737.7x + 5.198$ | 0.9822 | 0.44 |
| Average | 46.7 | 3.29 | | | 0.45 |

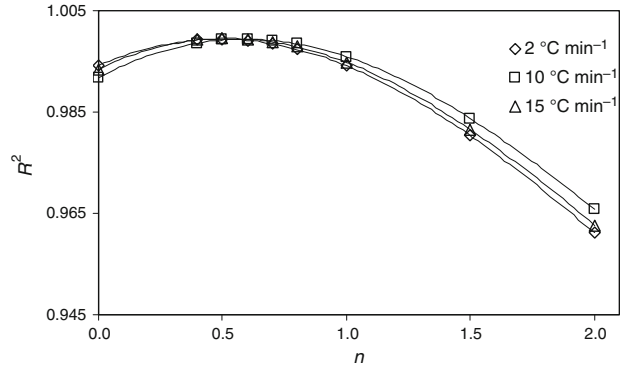


**Fig. 4** $R^2$–$n$ curves obtained by Coats–Redfern method

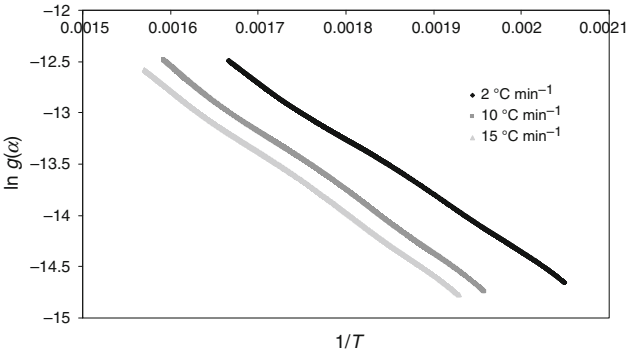


**Fig. 5** lng(α) versus (1/$T$) plot for Coats–Redfern method

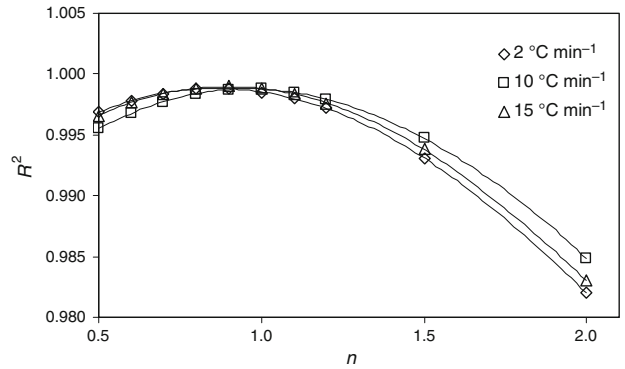


**Fig. 6** $R^2$–$n$ curves obtained by Horowitz–Metzger method

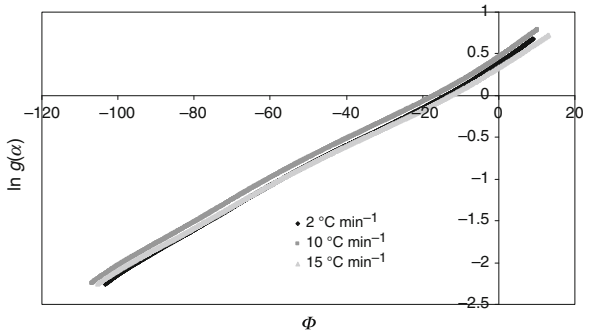


**Fig. 7** lng(α) versus $\Phi$ plot for Horowitz–Metzger method

**Table 5** Kinetic parameters calculated from Horowitz–Metzger method

| $B$/°C min$^{-1}$ | $E$/ kJ mol$^{-1}$ | Log $A$/ min$^{-1}$ | Plot Equation | $R^2$ | $n$ |
|---|---|---|---|---|---|
| 2 | 72.4 | 5.26 | $y = 0.0249x + 0.384$ | 0.9988 | 0.86 |
| 10 | 78.4 | 6.23 | $y = 0.0247x + 0.460$ | 0.9988 | 0.96 |
| 15 | 78.0 | 6.24 | $y = 0.0241x + 0.345$ | 0.9990 | 0.90 |
| Average | 76.3 | 5.91 | | | 0.91 |

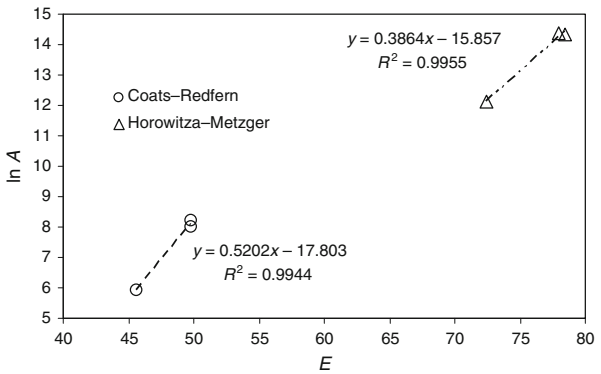


**Fig. 8** Kinetic compensation effect for walnut shell

Considering the results tabulated in Tables 3, 4, and 5, it can be said that kinetic parameter values were affected from the variations in heating rates. Increasing the heating rate from 2 to 10 °C min$^{-1}$ led to an increase in activation energy and pre-exponential factor values. Further

**Table 4** Kinetic parameters calculated from Coats–Redfern method

| $B$/°C min$^{-1}$ | $E$/kJ mol$^{-1}$ | Log $A$/min$^{-1}$ | Plot equation | $R^2$ | $n$ |
|---|---|---|---|---|---|
| 2 | 45.6 | 2.57 | $y = -5485.1x - 3.386$ | 0.9994 | 0.49 |
| 10 | 49.8 | 3.48 | $y = -5992.2x - 2.981$ | 0.9993 | 0.59 |
| 15 | 49.8 | 3.56 | $y = -5992.6x - 3.195$ | 0.9995 | 0.52 |
| Average | 48.4 | 3.20 | | | 0.53 |

increment of heating rate to 15 °C $min^{-1}$ did not reflect a considerable change in activation energy and pre-exponential factor values calculated from Coats–Redfern and Horowitz–Metzger method. For the results obtained from Arrhenius method, an increasing trend was observed with increasing heating rate. In every case, the relationship between the activation energy and pre-exponential factor was linear. In literature, this situation is called as "kinetic compensation effect," and defined as "a rise in $E$ (which will decrease the rate of reaction at any particular temperature) is partially or completely offset by an increase in $A$" [23]. In many cases, the variation of these parameters corresponds to the equation $\ln A = a + bE$, where $a$ and $b$ are constants. As shown in Fig. 8, kinetic compensation effect was obviously present in this study.

## Conclusions

Non-isothermal TG analyses of walnut shell samples have been carried out in 50–800 °C temperature range at 2, 10, and 15 °C $min^{-1}$ heating rates under nitrogen flow (50 mL $min^{-1}$). Three distinct mass loss zones were determined. These zones were attributed to removal of water, decomposition of hemicellulose + cellulose and decomposition of lignin, respectively. Most of the mass loss (~56%) had occurred in second zone which was referred as active pyrolysis zone. It was found that 60% pyrolysis conversion (based on volatiles) rates can be achieved at relatively low temperatures (~380 °C). Based on this result, walnut shell was found to have considerable potential for pyrolysis processes.

Kinetic parameters of active pyrolysis zone were calculated by using Arrhenius, Coats–Redfern, and Horowitz–Metzger methods. Activation energy, pre-exponential factor (logarithmic), and reaction order values were found between the intervals of 45.6–78.4 kJ $mol^{-1}$, 2.57–6.24 $min^{-1}$, and 0.44–0.96, respectively. Arrhenius and Coats–Redfern methods showed great agreement while Horowitz–Metzger method yielded relatively higher values. The results showed the existence of kinetic compensation effect clearly.

**Acknowledgements** The author is grateful to Işık Yavuz for her valuable help during the analyses. The author would also like to thank Dr. Dilek Duranoğlu and Prof. Dr. Esen Bolat for their continuous support during the studies.

## References

1. IEA. World energy outlook. Paris: OECD/IEA; 2008.
2. Bassam NE. Handbook of energy crops: a complete reference to species, development and applications. UK: Earthscan; 2010.
3. Karaca F, Bolat E. Coprocessing of a Turkish lignite with a cellulosic waste material 1. The effect of coprocessing on liquefaction yields at different reaction temperatures. Fuel Process Technol. 2000;64:47–55.
4. Naik S, Goud VV, Rout PK, Jacobson K, Dalai AK. Characterization of Canadian biomass for alternative renewable fuel. Renew Energy. 2010;35:1624–31.
5. Bridgwater AV, Peacocke GVC. Fast pyrolysis processes for biomass. Renew Sustain Energy Rev. 2000;4:1–73.
6. Senneca O. Kinetics of pyrolysis, combustion and gasification of three biomass fuels. Fuel Process Technol. 2007;88:87–97.
7. Bahng M-K, Mukarakate C, Robichaud DJ, Nimlos MR. Current technologies for analysis of biomass thermochemical processing: a review. Anal Chim Acta. 2009;651:117–38.
8. Yaman S. Pyrolysis of biomass to produce fuels and chemical feedstocks. Energy Convers Manag. 2004;45:651–71.
9. García-Ibañez P, Sánchez M, Cabanillas A. Thermogravimetric analysis of olive-oil residue in air atmosphere. Fuel Process Technol. 2006;87(2):103–7.
10. Sharma A, Rao TR. Kinetics of pyrolysis of rice husk. Bioresour Technol. 1999;67:53–9.
11. Alvarez VA, Vázquez A. Thermal degradation of cellulose derivatives/starch blends and sisal fibre biocomposites. Polym Degrad Stab. 2004;84:13–21.
12. Janković B, Adnadević B, Jovanović J. Non-isothermal kinetics of dehydration of equilibrium swollen poly(acrylic acid) hydrogel. J Therm Anal Calorim. 2005;82:7–13.
13. Yang H, Yan R, Chen H, Lee DH, Zheng C. Characteristics of hemicelluloses, cellulose and lignin pyrolysis. Fuel. 2007;86:1781–8.
14. Idris SS, Rahman NA, Ismail K, Alias AB, Rashid ZA, Aris MJ. Investigation on thermochemical behaviour of low rank Malaysian coal, oil palm biomass and their blends during pyrolysis via thermogravimetric analysis (TGA). Bioresour Technol. 2010;101:4584–92.
15. Blasi CD. Modeling chemical and physical processes of wood and biomass pyrolysis. Progr Energy Combust. 2008;34:47–90.
16. Wu Y-M, Zhao Z-L, Li H-B, He F. Low temperature pyrolysis characteristics of major components of biomass. J Fuel Chem Technol. 2009;37(4):427–32.
17. Zapata B, Balmesada J, Fragoso-Israel E, Torres-García E. Thermo-kinetics study of orange peel in air. J Therm Anal Calorim. 2009;98:309–15.
18. Souza BS, Moreira APD, Teixeira AMRF. TG-FTIR coupling to monitor the pyrolysis products from agricultural residues. J Therm Anal Calorim. 2009;97:637–42.
19. Aboulkas A, El Harfi K, El Bouadili A. Pyrolysis of olive residue/low density polyethylene mixture: part I thermogravimetric kinetics. J Fuel Chem Technol. 2008;36(6):672–8.
20. Lapuerta M, Hernández JJ, Rodríguez J. Kinetics of devolatilisation of forestry wastes from thermogravimetric analysis. Biomass Bioenergy. 2004;27:385–91.
21. Ebrahimi-Kahrizsangi R, Abbasi MH. Evaluation of reliability of Coats-Redfern method for kinetic analysis of non-isothermal TGA. Trans Nonferrous Met Soc China. 2008;18:217–21.
22. Aly AAM, Osman AH, El-Mottaleb MA, Gouda GAH. Thermal stability and kinetic studies of cobalt (II), nickel (II), copper (II), cadmium (II) and mercury (II) complexes derived from *n*-salicylidene Schiff bases. J Chil Chem Soc. 2009;54(4):349–53.
23. L'vov BV. Thermal decomposition of solids and melts: new thermochemical approach to the mechanism, kinetics and methodology. Dordrecht, The Netherlands: Springer; 2007.